Bulletin of Glaciological Research 32 (2014) *47–53*
doi: http://dx.doi.org/10.5331/bgr.32.47

Article

Effects of temperature and grain type on time variation of snow specific surface area

Akihiro HACHIKUBO[1]*, Satoru YAMAGUCHI[2], Hayato ARAKAWA[3], Tomonori TANIKAWA[4], Masahiro HORI[4], Konosuke SUGIURA[5], Sumito MATOBA[6], Masashi NIWANO[7], Katsuyuki KUCHIKI[7] and Teruo AOKI[7]

1 Environmental and Energy Resources Research Center, Kitami Institute of Technology, Kitami 090–8507, Japan
* hachi@mail.kitami-it.ac.jp
2 Snow and Ice Research Center, National Research Institute for Earth Science and Disaster Prevention, Nagaoka 940–0821, Japan
3 YAGAI-KAGAKU Co., Ltd., Sapporo 065–0043, Japan
4 Earth Observation Research Center, Japan Aerospace Exploration Agency, Tsukuba 305–8505, Japan
5 Center for Far Eastern Studies, University of Toyama, Toyama 930–8555, Japan
6 Institute of Low Temperature Science, Hokkaido University, Sapporo 060–0819, Japan
7 Meteorological Research Institute, Tsukuba 305–0052, Japan

(Received November 13, 2013; Revised manuscript received April 14, 2014)

Abstract

The specific surface area (SSA) of snow is of particular interest to researchers because SSA is strongly related to snow albedo and is a comparatively better indicator of snow's complexity than grain size. The time variation of SSA for fresh snow samples was observed in the laboratory under isothermal conditions at 226 K and 254 K using the gas adsorption method and Brunauer–Emmett–Teller theory. The SSA of the snow samples decreased with time under isothermal metamorphism. The decrease in SSA was fitted with the logarithmic equation proposed by Legagneux *et al.* (2003), and adjustable parameters were obtained. The rate of decrease in SSA depended on the shape of the initial snow type and temperature. Dendritic snow samples exhibited large initial SSAs, and their SSAs decreased faster compared with those of fragmented (collected from drifting snow) and plate-like precipitation particles with relatively small initial SSAs. The rate of decrease in SSA was lower at 226 K than that at 254 K.

Key words: SSA, BET theory, gas adsorption, methane

1. Introduction

Snow albedo is determined by the scattering of light in a snow medium, which is a function of grain size, shape and the concentration of impurities (Warren, 1982). The grain size of a snow particle is one of the important physical parameters of snow that strongly affects the near-infrared (NIR) albedo (Wiscombe and Warren, 1980). Because snow particles have complex shapes and can aggregate, it is difficult to define snow grain size. For example, in a recent study, snow grain size r_2 was defined as one half of the branch width of dendrites or one half of the width of the narrower part of broken crystals, corresponding to the optically equivalent snow grain radius (Aoki *et al.*, 2000; 2003; 2007). The minimum, mode and maximum values of r_2 in each snow layer were recorded using a handheld lens with a scale; however, the values of r_2 showed wide distribution and varied among observers.

The specific surface area (SSA) of snow is related to the radiative properties of snow and is a comparatively better indicator of snow's complexity than grain size (Domine *et al.*, 2006). SSA is defined as the ratio between the surface area [m^2] and unit mass [kg]. A procedure to measure the SSA of snow using the gas adsorption method and Brunauer–Emmett–Teller (BET) theory (Brunauer *et al.*, 1938) has been developed and applied (Chaix *et al.*, 1996; Dominé *et al.*, 2001; Legagneux *et al.*, 2002). In these studies, methane was observed to be a suitable adsorption gas for measuring the SSA of snow, as methane has a much lower vapor pressure than nitrogen, the usual adsorbent. Therefore, the relative pressure drop during adsorption is much greater than that for nitrogen, and this allows the measurement of porous solids with low SSAs, such as snow. Nitrogen has been used successfully for high SSA solids, such as clays and catalysts, but is very difficult to use for snow.

Legagneux *et al.* (2002) measured SSA values of snow from 10.0 $m^2 kg^{-1}$ to 158.0 $m^2 kg^{-1}$. Cabanes *et al.* (2003) measured the decrease in the SSA of snow layers in the Arctic region and the French Alps and fitted the decrease to an exponential equation as a function of temperature. However, the decrease of natural snow's

Table 1. List of snow samples.

Sample	Sampling date	Initial crystal types	Temperature [K]
No.1	Feb 09, 2013	Fragmented precipitation particles	254
No.2	Feb 23, 2013	Dendritic crystals coated with rime	226
No.3	Mar 16, 2013	Dendritic crystals	254
No.4	Mar 20, 2013	Plate-like crystals	226
No.5	Jan 31, 2014	Dendritic crystals coated with rime	254
No.6	Jan 31, 2014	Dendritic crystals coated with rime	226

SSA was affected by meteorological factors; apparently, the wind effect enhanced the decrease in SSA. The SSA of snow monotonically decreases with time under isothermal conditions and is expressed by an empirical logarithmic equation (Legagneux *et al.*, 2003; 2004). Taillandier *et al.* (2007) revealed that the rate of decrease in SSA under a temperature gradient was faster than that under isothermal metamorphism. However, Domine *et al.* (2009) reported some exceptions: depth hoar formed from melt–freeze crust and wind effects on the sieving of blowing snow particles eventually increased SSA. Therefore, the wind has opposing roles: decreasing the SSA by enhancing metamorphism and increasing the SSA by supplying fine snow particles generated by blowing and drifting snow. We need to accumulate data on SSA changes to construct a numerical snowpack model and predict the SSA values (Morin *et al.*, 2013).

The rate of decrease in SSA has been measured at high temperature ranges in previous studies: Taillandier *et al.* (2007) summarized the rate of decrease in SSA from 254 K to 269 K. However, it is important to be able to predict the change of surface snow's SSA in the polar regions. The surface temperatures of inland Greenland (Kobashi *et al.*, 2011) and Antarctica (Motoyama *et al.*, 2005) are approximately 243 K and 218 K, respectively; however, the rate of decrease in SSA below 253 K has not been reported so far.

The SSA of snow has been measured directly by not only the gas adsorption method but also stereology (Narita, 1969; 1971; Arakawa *et al.*, 2009) and X-ray microtomography (Flin *et al.*, 2005; Kerbrat *et al.*, 2008) and indirectly by optical methods using NIR (Matzl and Schneebeli, 2006) and short-wave infrared (SWIR; Gallet *et al.*, 2009) photometry of snow. The methods of stereology and X-ray microtomography inherently have low resolution and underestimate the SSA for fine particles such as fresh snow. The optical NIR and SWIR methods have been recently developed and have the advantage of short measurement times. Although the gas adsorption method takes several hours to obtain a value and requires liquid nitrogen, it is still useful for validation because it directly measures the SSA.

In this study, we constructed a system for measuring the SSA of snow using the gas adsorption method according to Legagneux *et al.* (2002). We collected fresh snow (precipitation particles) samples from Kitami (eastern Hokkaido, Japan) and stored them in cold rooms (226 K and 254 K) to determine the processes causing a decrease in SSA under isothermal conditions. Furthermore, we examined the effects of temperature and crystal shape on the time variation of the SSA.

2. Experimental methods

2.1 Snow samples

Table 1 lists the six natural snow samples used in this experiment. Precipitation particles were collected from Kitami, Japan (43°49′26″N, 143°54′12″E and 86 m above sea level) and stored for long periods (50–230 days) in cold rooms, where the temperatures were controlled at 226 K and 254 K. The temperatures of samples were controlled with an accuracy of ±0.1 K. Sample No. 1 was fragmented particles collected from drifting snow on February 09, 2013 with a relatively smaller crystal size than the other samples. Samples No. 2 and No. 3 were dendritic crystals and rimes adhered to the former. Sample No. 4 was plate-like precipitation particles. Samples No. 5 and No. 6 were rimed dendritic crystals collected on the same day (January 31, 2014). Each of these samples was stored in a plastic bag within a thermally insulated box. The photographs of the snow particles were taken when the measurement of SSA was conducted.

2.2 Apparatus and methods

The schematic view of the instrument for measuring the snow SSA is shown in Fig. 1. The method and principles of the gas adsorption method have been described in detail by Legagneux *et al.* (2002). The main device is composed of helium and methane tanks (50 mL each), two pressure cells for the sample (30 mL) and reservoir (50 mL), a manometer (Baratron® 722B, MKS Instruments) and greaseless valves connected with tubes made of stainless steel and Swagelok® fittings. The accuracy of the manometer was 0.5 %. The basic performance of the device has been reported by Hachikubo *et al.* (2012; 2013) with measurement repeatability of 3 % (standard deviation).

Approximately 10 g of a snow sample was placed into a sample cell and immersed in liquid nitrogen to maintain the temperature at 77 K. The sample cell was connected to the main device and placed under vacuum. Methane introduced into the reservoir cell via valves V_1, V_3, V_4 and V_5 was diffused into the sample cell through valve V_7 and was partly adsorbed on the surface of snow particles. The adsorbed amount was calculated by comparison with the result using helium because helium is not adsorbed on snow particles' surfaces. We obtained a dataset of the relation between the amount of methane adsorption and the pressure of methane. We applied the BET theory to obtain the surface area of the sample and the heat of the adsorption of methane on the ice surface.

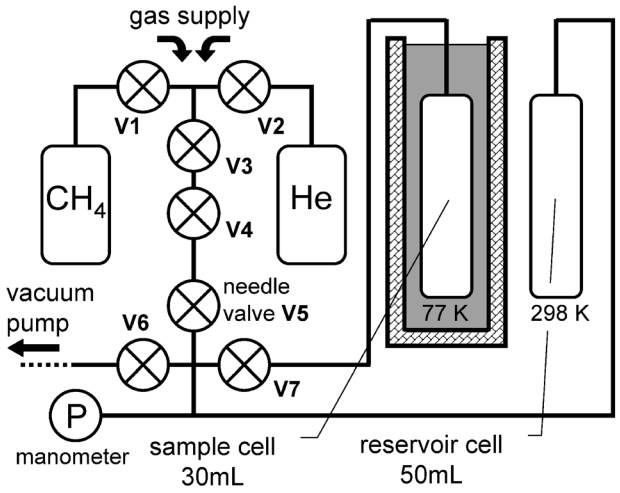

Fig. 1. Schematic view of the apparatus for measuring SSA of snow. P: pressure gauge, V_{1-7}: ball valves and a needle valve. The pressures of helium and methane reduce step-by-step through the valves V_{3-5}.

We adopted 0.1918 nm^2 as the molecular cross-sectional surface area of methane on ice (Chaix *et al.*, 1996) and 1,294 Pa as the vapor pressure of methane at 77 K (Legagneux *et al.*, 2002). We measured the surface area of the sample cell (2.34×10^{-2} m^2) by the same methane adsorption and subtracted it from the measured data, because Legagneux *et al.* (2004) and Domine *et al.* (2007) reported that the adsorption of methane on the inner wall of the sample cell was not negligible.

3. Results and discussion

Fig. 2 shows examples of the BET plots. The BET transform is expressed as a function of P/P_0:

$$\frac{P}{V(P_0-P)}=\frac{1}{V_mC}+\left(\frac{C-1}{V_mC}\right)\left(\frac{P}{P_0}\right), \quad (1)$$

where P and P_0 are the pressure of methane at each isotherm and its vapor pressure at 77 K, respectively, V is the volume of total adsorption, V_m is the monolayer adsorption capacity, and C is the constant related to the heat of adsorption. According to Eq. (1), the slope and intercept of the BET plots in Fig. 2 provide V_m and C. Linear relations were obtained in the P/P_0 range of 0.07–0.20, and the corresponding correlation coefficients exceeded 0.999. The SSA values of samples No. 1–6 were determined to be 53.1, 74.3, 87.9, 54.9, 79.7 and 73.1 [$m^2\,kg^{-1}$], respectively. The heats of adsorption were calculated as 2,552; 2,521; 2,667; 2,557; 2,722 and 2,576 [J mol^{-1}], respectively; these values were within the range of 2,540±200 [J mol^{-1}] as reported by Domine *et al.* (2007).

The processes of isothermal metamorphism are shown in Fig. 3. Isothermal sintering progressed and

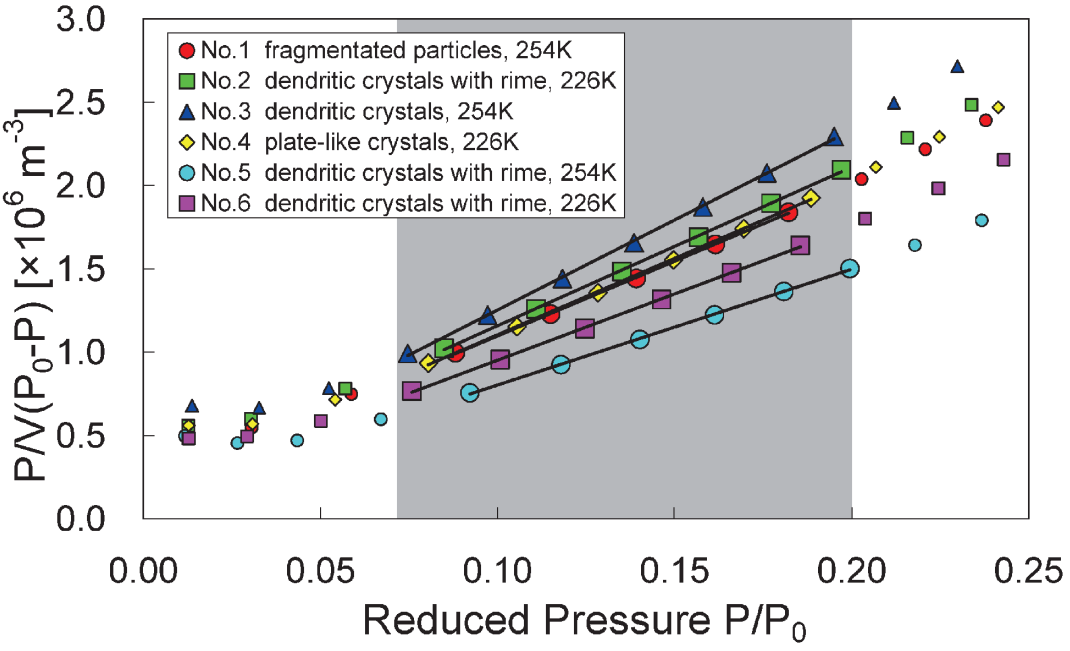

Fig. 2. BET plots of the isotherm of samples No. 1–6 at their first measurement. These data were obtained within a day after the snowfall. The linear relations appear in the P/P_0 range of 0.07–0.20 (shaded area).

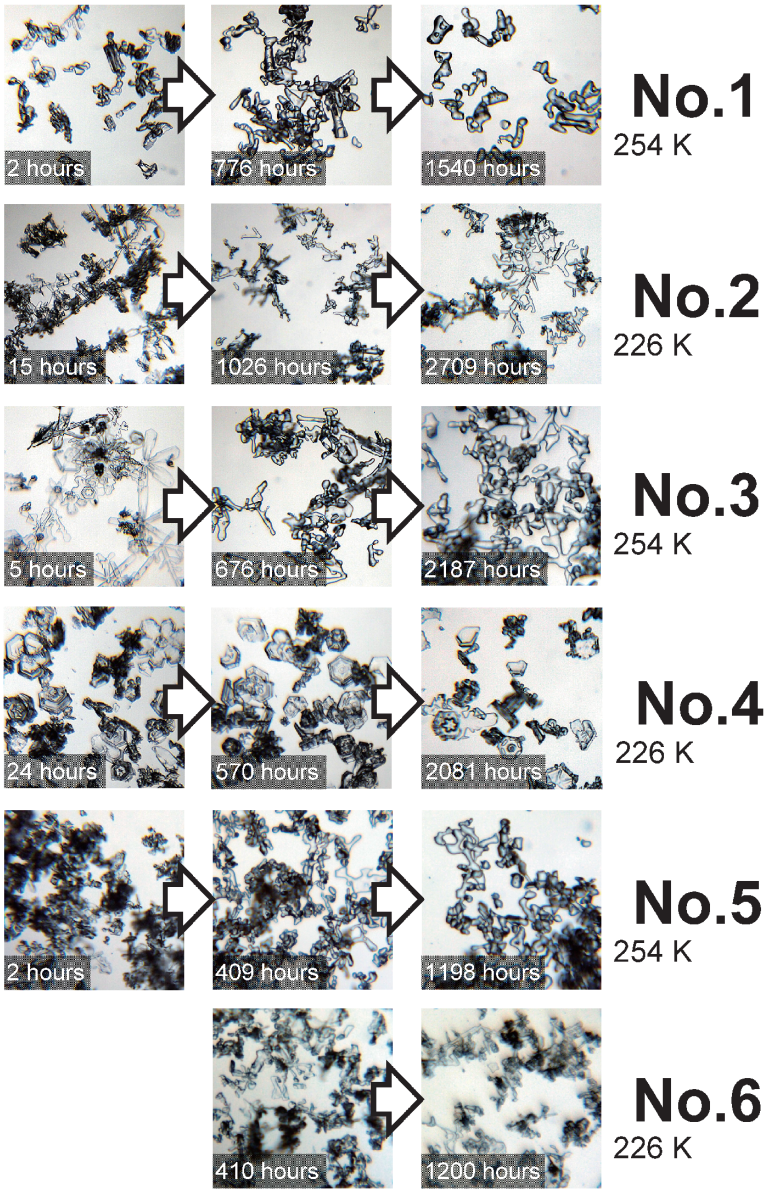

Fig. 3. Photographs of snow particles and their time variation. The size of each photograph is a 4 mm square. Initial snow types of sample No. 1, fragmented precipitation particles; sample No. 2, dendritic crystals coated with rime; sample No. 3, dendritic crystals; sample No. 4, plate-like crystals; samples No. 5 and No. 6, dendritic crystals coated with rime.

reduced the SSA of snow for all samples. Fragmented snow particles (sample No. 1, 254 K) changed quickly to small, rounded crystals. In contrast, plate-like crystals (sample No. 4, 226 K) retained their shape for more than 2,000 h at low temperature. The complicated branches of the dendrites were well preserved in samples No. 2 and No. 3; the former, which was rimed, was better preserved at 226 K. Samples No. 5 and No. 6 were originally the same precipitations, but the latter was well preserved at low temperature.

Fig. 4 shows the time variation of SSA; SSA decreased with time in all samples. Although samples No. 1, No. 3 and No. 5 had the same temperature (254 K), the rate of decrease in SSA was different for each: the SSA of sample No. 3 (dendritic crystals) decreased faster than that of samples No. 1 and No. 5. Samples No. 2 and No. 6 (dendritic crystals coated with rime) and No. 4 (plate-like crystals) had a lower temperature (226 K), and the rate of SSA decrease in sample No. 4 was smaller than those of samples No. 1, No. 3 and No. 5. The rate of SSA decrease in samples No. 2 and No. 6 was close to that in sample No. 1, despite samples No. 2 and No. 6 being preserved at a lower temperature. These results can be explained by the fact that the SSA of the dendritic crystals decreased relatively faster than that of the other samples of different shapes. Therefore, it is evident that the rate of SSA decrease depends on not only the temperature but also the initial shape of the precipitation particles. The SSAs of fragmented particles generated under windy conditions and plate-like crystals that typically formed under low humidity decreased slowly, whereas those of dendritic crystals decreased quickly. Although rimed particles contributed to a large SSA (Cabanes *et al.*, 2002), the effect of rime on the change of

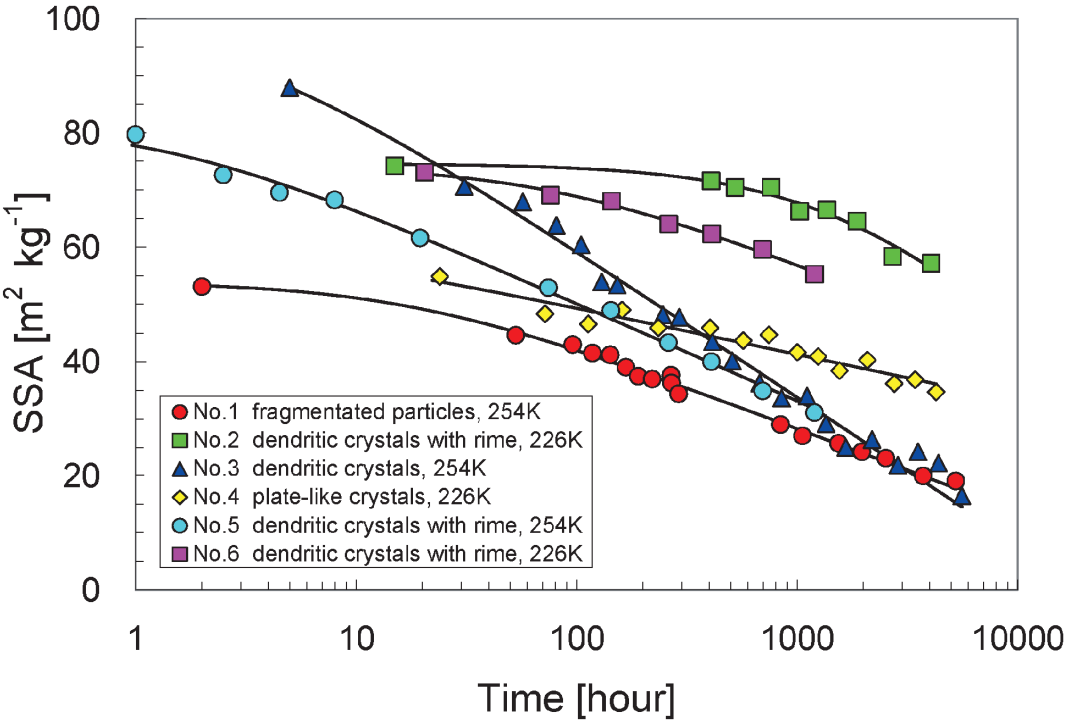

Fig. 4. Time variation of SSA of the six precipitation particles (samples No. 1–6). The solid lines express their fitted curves according to Legagneux *et al.* (2003).

SSA of samples No. 2, No. 5 and No. 6 needs further consideration.

Legagneux *et al.* (2003) proposed an empirical equation for the time variation of snow SSA:

$$SSA = -A\log(t+\Delta t)+B, \quad (2)$$

where A, B and Δt (change in time) are the fitting parameters. These parameters for samples No. 1–6 are summarized in Table 2. The fitting parameters A and B relate to the rate of decrease in SSA and the initial SSA, respectively. Furthermore, Legagneux *et al.* (2003) suggested an empirical linear relationship between A and B for a given temperature, as shown in Fig. 5. The fitted lines at 254 K and 226 K are plotted as red and green bold lines, respectively. As snow metamorphism is faster at higher temperatures, the line was upshifted from 226 K to 254 K. The rate of decrease, under the same initial SSA, was greater at higher temperatures. The black solid line in Fig. 5 shows data obtained under isothermal conditions from a previous study (mixed data at 258 K, 263 K and 269 K; Taillandier *et al.*, 2007), which nearly overlapped the fitted line for our data at 254 K; however, the value of parameter A was slightly higher because of the higher temperatures employed in the aforementioned study. Therefore, the relationship between A and B in our data agree well with that from the previous study. The broken line in Fig. 5 shows the relationship between A and B under a temperature gradient (Taillandier *et al.*, 2007); it was upshifted from the solid line obtained under isothermal conditions because the decrease in SSA was faster under the temperature gradient than isothermal conditions.

Table 2. Fitting parameters of the Eq. (2).

Sample	A [m^2 kg^{-1}]	B [m^2 kg^{-1}]	Δt [hour]
No.1	6	72	18
No.2	15	190	1788
No.3	11	111	2
No.4	4	66	4
No.5	7	84	1
No.6	7	104	79

Questions regarding the determination of the other fitting parameter Δt remain. Legagneux *et al.* (2003) proposed the idea that the value of B was close to the initial SSA, and the value of A could be derived from the relationship between A and B, as shown in Fig. 5; however, Δt could not be determined. Taillandier *et al.* (2007) noted that the effect of Δt on the fitting was small, as they showed that most data for Δt were within 1 day. On the contrary, Δt of samples No. 2 and No. 6 seemed to be large (up to several tens of days, Table 2). The SSA of sample No. 2 was almost constant during the first 14–400 h (Fig. 4) and then decreased. Legagneux *et al.* (2004) showed that Eq. (2) is an approximation of the Ostwald ripening theory, which expresses the coarsening of grains. In the early stages of snow metamorphism, the rate of decrease in SSA was relatively small (Fig. 4 Legagneux *et al.*, 2004) compared with Eq. (2). Possibly, low temperature and crystal shape affected the rate of decrease in SSA, and Δt increased to fit Eq. (2). On the

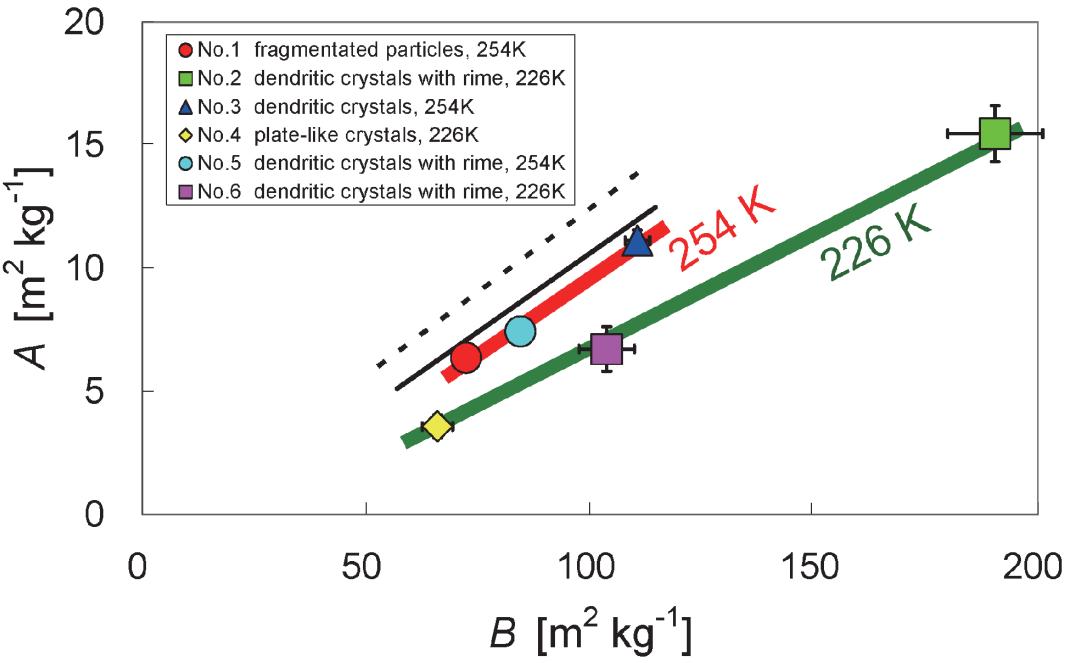

Fig. 5. Relation between the fitting parameters A and B of Eq. (2). Red and green bold lines show the relations at 254 K and 226 K, respectively. Broken and solid lines show the relations of the temperature gradient and isothermal data, respectively (Taillandier *et al.*, 2007).

other hand, Legagneux and Domine (2005) showed that the rate of decrease in SSA under isothermal conditions depends on the distribution of the radii of curvature (DRC). Because the SSA of snow with a narrow DRC decreases more slowly (Legagneux and Domine, 2005), sample No. 2 probably had a narrow DRC. Future work needs to investigate the application range of Eq. (2) in which Δt is negligible.

4. Concluding remarks

We measured the time variation of the SSA of snow under isothermal conditions. Even when samples were stored at the same temperature, the rate of decrease in SSA depended on the type of precipitation particles, which determined their initial SSA. We obtained the fitting parameters of Eq. (2) according to Legagneux *et al.* (2003) and observed that our data agreed well with their results. At the lower temperature (226 K), the parameter A, corresponding to the rate of decrease in SSA, was smaller than that obtained at 254K. We clearly demonstrated the effect of temperature on the decreasing rate of SSA. Although the temperature of 226 K is much lower than that of seasonal snow around the world, it is relevant to the snow on the ice sheets in the polar regions. Therefore, the results of this study indicated that Eq. (2) can be applied to estimate the change of surface snow's SSA on the Greenland and Antarctic ice sheets. Although Eq. (2) is valid in the time range of less than 1 day to about 150 days (Taillandier *et al.*, 2007), the limit of application under low temperatures (less than 254 K) is still unknown. To express the time variation of SSA as a function of time and temperature, further data need to be collected. The data describing the SSA decrease under a temperature gradient are also insufficient. Furthermore, prediction of the initial SSA will be an important research target for constructing an improved numerical snowpack model.

Acknowledgments

We are grateful to Dr. H. Sakagami of Kitami Institute of Technology for his helpful suggestions to construct the SSA measuring device. We also thank Mr. K. Fujita of the Institute of Low Temperature Science for the development of the sample chamber and snow sampler. This work was supported by the Japan Society for the Promotion of Science (JSPS) KAKENHI Grant Number 23221004, and the Grant for Joint Research Program of the Institute of Low Temperature Science, Hokkaido University, proposal No. 2013-12.

References

Aoki, Te., Aoki, Ta., Fukabori, M., Hachikubo, A., Tachibana, Y. and Nishio, F. (2000): Effects of snow physical parameters on spectral albedo and bidirectional reflectance of snow surface. *J. Geophys. Res.*, **105**, 10219–10236, doi:10.1029/1999JD901122.

Aoki, T., Hachikubo, A. and Hori, M. (2003): Effects of snow physical parameters on broadband albedos. *J. Geophys. Res.*, **108**, 4616, doi:10.1029/2003JD003506.

Aoki, T., Hori, M., Motoyoshi, H., Tanikawa, T., Hachikubo, A., Sugiura, K., Yasunari, T. J., Storvold, R., Eide, H. A., Stamnes, K., Li, W., Nieke, J., Nakajima, Y. and Takahashi, F. (2007): ADEOS-II/GLI snow/ice products: Part II—Validation results using GLI and MODIS data. *Remote Sens. Environ.*, **111**, 274–290, doi:10.1016/j.rse.2007.02.035.

Arakawa, H., Izumi, K., Kawashima, K. and Kawamura, T. (2009): Study on quantitative classification of seasonal snow using

specific surface area and intrinsic permeability. *Cold Reg. Sci. Tech.*, **59**, 163–168, doi:10.1016/j.coldregions.2009.07.004.

Brunauer, S., Emmet, P. H. and Teller, E. (1938): Adsorption of gases in multimolecular layers. *J. Am. Chem. Soc.*, **60**, 309–319, doi:10.1021/ja01269a023.

Cabanes, A., Legagneux, L. and Dominé, F. (2002): Evolution of the specific surface area and of crystal morphology of Arctic fresh snow during the ALERT 2000 campaign. *Atmos. Environ.*, **36**, 2767–2777, doi:10.1016/S1352-2310(02)00111-5.

Cabanes, A., Legagneux, L. and Dominé, F. (2003): Rate of evolution of the specific surface area of surface snow layers. *Environ. Sci. Technol.*, **37**, 661–666, doi:10.1021/es025880r.

Chaix, L., Ocampo, J. and Dominé, F. (1996): Adsorption of CH_4 on laboratory-made crushed ice and on natural snow at 77 K: Atmospheric implications. *C. R. Acad. Sci., Ser. IIa*, **322**, 609–616.

Dominé, F., Cabanes, A., Taillandier, A. -S. and Legagneux, L. (2001): Specific surface area of snow samples determined by CH_4 adsorption at 77 K and estimated by optical microscopy and scanning electron microscopy. *Environ. Sci. Technol.*, **35**, 771–780, doi:10.1021/es001168n.

Domine, F., Salvatori, R., Legagneux, L., Salzano, R., Fily, M. and Casacchia, R. (2006): Correlation between the specific surface area and the short wave infrared (SWIR) reflectance of snow. *Cold Reg. Sci. Tech.*, **46**, 60–68, doi:10.1016/j.coldregions.2006.06.002.

Domine, F., Taillandier, A. -S. and Simpson, W. R. (2007): A parameterization of the specific surface area of seasonal snow for field use and for models of snowpack evolution. *J. Geophys. Res.*, **112**, F02031, doi:10.1029/2006JF000512.

Domine, F., Taillandier, A. -S., Cabanes, A., Douglas, T. A. and Sturm, M. (2009): Three examples where the specific surface area of snow increased over time. *The Cryosphere*, **3**, 31–39, doi:10.5194/tc-3-31-2009.

Flin, F., Brzoska, J. B., Coeurjolly, D., Pieritz, R. A., Lesaffre, B., Coléou, C., Lamboley, P., Teytaud, O., Vignoles, G. L. and Delesse, J. F. (2005): Adaptive estimation of normals and surface area for discrete 3-D objects: Application to snow binary data from X-ray tomography, *IEEE Trans. Image Process.*, **14**, 585–596, doi:10.1109/TIP.2005.846021.

Gallet, J. -C., Domine, F., Zender, C. S. and Picard, G. (2009): Measurement of the specific surface area of snow using infrared reflectance in an integrating sphere at 1310 and 1550 nm. The *Cryosphere*, **3**, 167–182, doi:10.5194/tc-3-167-2009.

Hachikubo, A., Yamaguchi, S., Tanikawa, T., Hori, M., Sugiura, K., Niwano, M., Kuchiki, K. and Aoki, T. (2012): Development of the device for measuring snow specific surface area by gas adsorption. *Snow and Ice in Hokkaido (a bulletin of the Hokkaido branch, Japanese Society of Snow and Ice)*, **31**, 45–48. (in Japanese)

Hachikubo, A., Yamaguchi, S., Arakawa, H., Tanikawa, T., Hori, M., Sugiura, K., Niwano, M., Kuchiki, K. and Aoki, T. (2013): Investigation of adsorbent for a measurement of snow specific surface area by the gas-adsorption method. *Proceedings International Snow Science Workshop*, 7–11 October, 2013, Grenoble, France, 73–77.

Kerbrat, M., Pinzer, B., Huthwelker, T., Gäggeler, H. W., Ammann, M. and Schneebeli, M. (2008): Measuring the specific surface area of snow with X-ray tomography and gas adsorption: comparison and implications for surface smoothness. *Atmos. Chem. Phys.*, **8**, 1261–1275, doi:10.5194/acp-8-1261-2008.

Kobashi, T., Kawamura, K., Severinghaus, J. P., Barnola, J.-M., Nakaegawa, T., Vinther, B. M., Johnsen, S. J. and Box, J. E. (2011): High variability of Greenland surface temperature over the past 4000 years estimated from trapped air in an ice core. *Geophys. Res. Lett.*, **38**, L21501, doi:10.1029/2011GL049444.

Legagneux, L., Cabanes, A. and Dominé, F. (2002): Measurement of the specific surface area of 176 snow samples using methane adsorption at 77 K. *J. Geophys. Res.*, **107**(D17), 4335, doi:10.1029/2001JD001016.

Legagneux, L., Lauzier, T., Dominé, F., Kuhs, W. F., Heinrichs, T. and Techmer, K. (2003): Rate of decay of the specific surface area of snow during isothermal experiments and morphological changes studied by scanning electron microscopy. *Can. J. Phys.*, **81**, 459–468, doi:10.1139/P03-025.

Legagneux, L., Taillandier, A. -S. and Domine, F. (2004): Grain growth theories and the isothermal evolution of the specific surface area of snow. *J. Appl. Phys.*, **95**, 6175–6184, doi:10.1063/1.1710718.

Legagneux, L. and Domine, F. (2005): A mean field model of the decrease of the specific surface area of dry snow during isothermal metamorphism. *J. Geophys. Res.*, **110**, F04011, doi:10.1029/2004JF000181.

Martzl, M. and Schneebeli, M. (2006): Measuring specific surface area of snow by near-infrared photography. *J. Glaciol.*, **52**, 558–564, doi:10.3189/172756506781828412.

Morin, S., Domine, F., Dufour, A., Lejeune, Y., Lesaffre, B., Willemet, J. -M., Carmagnola, C. M. and Jacobi, H. -W. (2013): Measurements and modeling of the vertical profile of specific surface area of an alpine snowpack. *Adv. Water Resour.*, **55**, 111–120, doi:10.1016/j.advwatres.2012.01.010.

Motoyama, H., Hirasawa, N., Satow, K. and Watanabe, O. (2005): Seasonal variations in oxygen isotope ratios of daily collected precipitation and wind drift samples and in the final snow cover at Dome Fuji Station, Antarctica. *J. Geophys. Res.*, **110**, D11106, doi:10.1029/2004JD004953.

Narita, H. (1969): Measurement of the specific surface of the deposited snow I. *Low Temp. Sci.*, **A27**, 77–86. (in Japanese with English summary)

Narita, H. (1971): Measurement of the specific surface of the deposited snow II. *Low Temp. Sci.*, **A29**, 69–79. (in Japanese with English summary)

Taillandier, A. -S., Domine, F., Simpson, W. R., Sturm, M. and Douglas, T. A. (2007): Rate of decrease of the specific surface area of dry snow: Isothermal and temperature gradient conditions. *J. Geophys. Res.*, **112**, F03003, doi:10.1029/2006JF000514.

Warren, S. G. (1982): Optical properties of snow. *Rev. Geophys. Space Phys.*, **20**, 67–89, doi:10.1029/RG020i001p00067.

Wiscombe, W. J. and Warren, S. G. (1980): A model for the spectral albedo of snow, I: Pure snow. *J. Atmos. Sci.*, **37**, 2712–2733, doi:10.1175/1520-0469(1980)037 <2712 : AMFTSA> 2.0.CO;2.